

PLANT SCIENCE

Launched at 36,000g

Johan L. van Leeuwen

Most mosses, including peat mosses of the genus *Sphagnum* (about 285 species), disperse their spores by turbulent wind (1). In still air, spores (22 to 45 μm in size) sink at only 0.5 to 2 cm/s, ideal for wind dispersal (2). However, spore capsules, positioned on a short stalk, grow to heights of about 1 cm and do not extend into the atmospheric turbulent boundary layer (more than 10 cm above ground). Peat mosses solve this problem with an “air gun” mechanism that explosively discharges spores from a pressurized cylindrical capsule ~ 2 mm in length (see the figure), projecting spores over 10 to 20 cm (1–3). On page 406 of this issue, Whitaker and

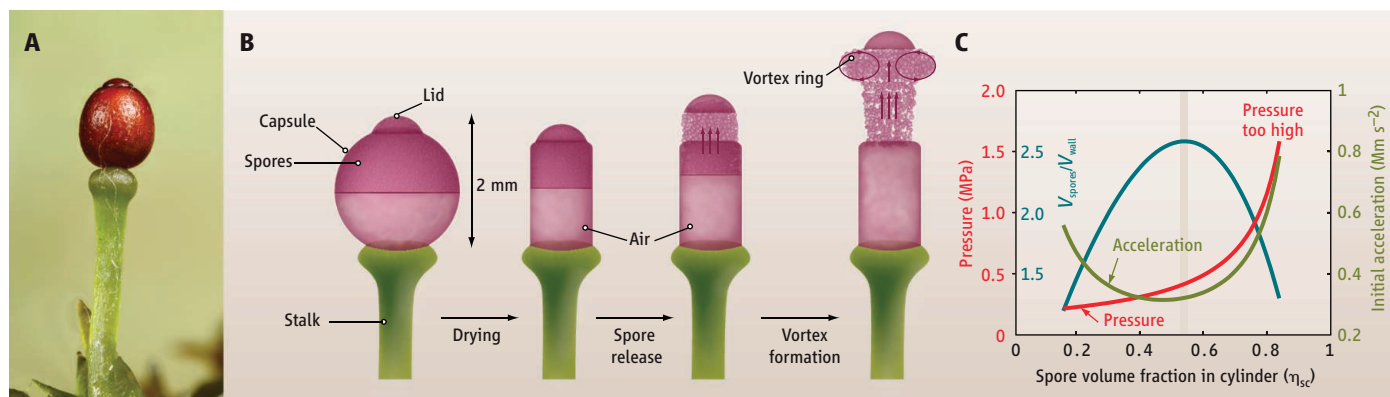
tial and even turbulent flow regime, enabling spores to travel long distances by entering the dynamics of a larger-scale vortex ring.

The power for the explosion stems from compressed air in the spore capsule. The intact mature capsule in peat mosses is spherical when wet. The upper portion of the capsule holds 20,000 to 240,000 spores (5), whereas the middle and lower portions contain air. As water evaporates from the epidermis through pores, the capsule transforms into a cylindrical shape of approximately the same height (1, 4, 6). The epidermal cells shrink, thus decreasing the circumference of the capsule. The final volume of the cylindrical capsule is only about three-eighths of

Peat mosses project thousands of spores in a turbulent vortex ring from a millimeter-sized pressurized cylindrical capsule.

the spores and traveling distance rises with increasing pressure and spore mass.

However, there is a price to pay for increased spore content, because the mechanical stress in the capsule wall is proportional to the internal pressure and inversely proportional to the wall thickness. Hence, wall thickness needs to increase linearly with pressure and thus nonlinearly with η_{sc} if wall stress is kept constant, which seems reasonable for identical material properties and a fixed safety factor for rupture. The required ratio of spore/wall volume (see the figure) has a skewed parabolic shape and peaks at about 2.6 for $\eta_{\text{sc}} = 0.54$, which is close to observed values of Whitaker and Edwards, and others (3, 4, 7). The multifaceted shape of



Spore discharge. (A) Spore capsule of *Sphagnum fimbriatum* on a short stalk. (B) The wet spherical capsule becomes cylindrical by drying. Quick release of the lid triggers spore discharge by internal air pressure. The jet of spores and air rolls up into a turbulent ring vortex that carries spores up to 15 to 20 cm. (C) Air pressure

(above ambient) rises nonlinearly with the volume fraction of spores (η_{sc}). Initial spore acceleration is highest for both low and high η_{sc} because of low spore mass or high pressure. $V_{\text{spores}}/V_{\text{wall}}$ is the spore/wall volume ratio. Vertical tan line corresponds to the predicted optimum in spore content, similar to observed η_{sc} (2–4).

Edwards (4) report that an upward-traveling turbulent vortex ring of spores and air is formed by this explosion within less than 0.2 ms, carrying sufficient momentum to reach the turbulent boundary layer.

The upward momentum of the air and spore mass determines the distance traveled by the spores. Whitaker and Edwards point out that the collective discharge of many spores is required to tip the aerodynamic balance from friction forces to inertial forces. A single spore projected at the same speed would decelerate so fast by viscous drag that it would travel only a few millimeters. The collective discharge of spores scales up the dynamics into the iner-

the original one, a reduction accomplished mainly by air compression. The change into an upright pressurized cylinder (see the figure) promotes vertical launch of the spores.

The volumes of air in the spherical (V_0) and cylindrical (V_1) states can be computed from the volume fraction of the spores (η_{sc}) and other tissues in the cylinder. Hence, air pressure in the cylinder (p_1) can be derived from Boyle's law ($p_0 V_0 = p_1 V_1 = \text{constant}$), setting p_0 equal to the ambient pressure. Even with the assumed isothermal conditions and taking $\eta_{\text{sc}} = 0.53$, as observed for *Sphagnum*, a pressure (relative to ambient) of about 400 kPa (5 atm absolute pressure) is estimated, which is similar to previous measurements (3). Air volume in the cylinder drops linearly with η_{sc} , but air pressure rises nonlinearly with η_{sc} . The momentum of

the spores promotes packing efficacy while reducing the sinking speed in air (relative to spheres of similar size).

The spore velocities recorded by Whitaker and Edwards (which was time-resolved with ultrahigh-speed videos of 10^4 to 10^5 frames per second) were as high as 30 m/s. Such velocities require very high accelerations because the travel distance within the tiny capsule is only a millimeter or less. The lid is presumably released through a combination of tension in the capsule wall (6, 7) and internal pressure, causing the sudden rupture of the relatively weak epidermal attachment ring, and enabling the upward acceleration of the spore mass by the vertical force of the compressed air (equal to air pressure times transverse area of the cylinder). Assuming that the compacted spores move initially as

one mass and applying Newton's second law (force equals mass times acceleration), one can calculate an initial acceleration of about $320,000 \text{ m/s}^2$ or $32,000g$ for a realistic η_{sc} of 0.54 and a density of the spores of 1200 kg/m^3 . Higher values of η_{sc} would lead to even higher accelerations. Whitaker and Edwards' movie S3 shows that the spore cloud progresses from rest by about 1.8 mm in 0.1 ms, representing an average speed of 18 m/s. If velocity increases linearly from rest, the actual speed is 36 m/s after 0.1 ms, resulting in an estimated acceleration of $360,000 \text{ m/s}^2$, 12.5% above the calculation.

The energy stored in the compressed air (about 0.27 mJ for $\eta_{sc} = 0.54$) is only partly

used to accelerate spores. As long as the air expands within the capsule, this energy mainly converts into kinetic energy of the spores. When most spores have left the capsule, relatively more energy converts into air convection, heat, and audible sound (2).

The upscaling principle elucidated by Whitaker and Edwards for peat moss has been exploited abundantly in nature for the dispersal of microscopic items, whether reproductive or waste products. Examples are found in other mosses, fungi (1), flowering plants [pollen dispersal (8)], and microscopic waste dispersal through water jets in filtering sponges and tunicates. We are only starting to discover and appreciate the wide array of unique solu-

tions devised by nature to enhance the dispersal of microscopic particles.

References

1. C. T. Ingold, *Spore Liberation* (Clarendon, Oxford, 1965).
2. S. Sundberg, *Ann. Bot.* **105**, 291 (2010).
3. S. Nawaschin, *Flora* **83**, 151 (1897).
4. D. L. Whitaker, J. Edwards, *Science* **329**, 406 (2010).
5. S. Sundberg, H. Rydin, *J. Bryol.* **20**, 1 (1998).
6. J. G. Duckett, S. Pressel, K. M. Y. P'ng, K. S. Renzaglia, *New Phytol.* **183**, 1053 (2009).
7. S. Sundberg, *New Phytol.* **185**, 886 (2010).
8. J. Edwards, D. Whitaker, S. Klionsky, M. J. Laskowski, *Nature* **435**, 164 (2005).

Supporting Online Material

www.sciencemag.org/cgi/content/full/329/5990/395/DC1
SOM Text

10.1126/science.1193047

PHYSICS

Pairs Rule Quantum Interference

James D. Franson

Quantum interference is one of the most mysterious features of quantum mechanics. In fact, Feynman referred to the double-slit interference experiment for single particles as the “only” mystery in quantum mechanics (1). On page 418 of this issue, Sinha *et al.* (2) describe a recent experiment that shows that quantum interference from a single photon arises only from pairs of possible paths through an interferometer. There is no need to invoke additional interference terms that might arise from interactions of three or more paths.

In classical mechanics, outcomes can be described directly with probabilities. In quantum mechanics, the probability of an outcome is obtained from probability amplitudes (wave functions) that may be negative or even take complex values. For example, if a single photon can traverse three possible paths through an interferometer to reach a detector, the different paths have probability amplitudes ψ_1 , ψ_2 , and ψ_3 (see the left-hand panel of the figure). The total probability amplitude ψ for the photon to reach the detector is the sum $\psi = \psi_1 + \psi_2 + \psi_3$, but this is not the probability P that the photon will reach the detector. Probability is calculated by taking the square of the probability amplitude as

$$P = |\psi|^2 = \psi^* \psi = |\psi_1 + \psi_2 + \psi_3|^2$$

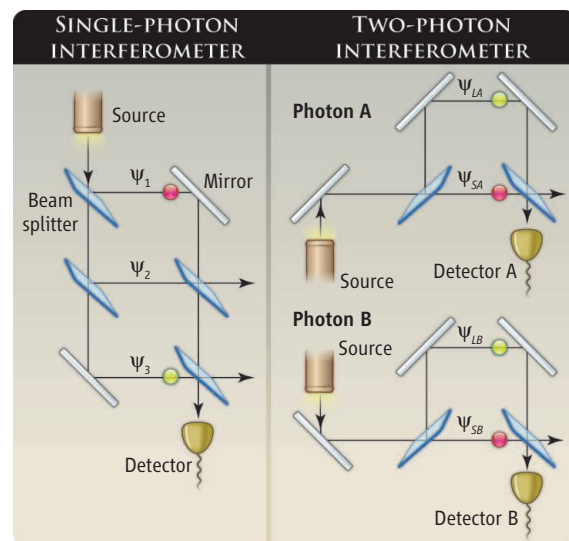
(the magnitude of the complex number ψ

is obtained by multiplying it by its complex conjugate ψ^*). Unlike the classical situation, where the individual probabilities would simply add, probability amplitudes can add constructively or cancel destructively. These interference effects depend on the phase shifts encountered in each path.

If a measurement had been made, it would have revealed which one of the three paths the photon took while it was traversing the interferometer. Nevertheless, a single photon must somehow determine the phase shift in all three paths to give the correct interference effects. This is the fundamental “mystery”

referred to by Feynman (1). The product of ψ^* and ψ is a series of terms of the form $\psi_i^* \psi_j$, so the detection probability should be determined by interference only between all possible pairs of paths through the interferometer (2). An example of such a pair of paths is indicated in the panel, left of the figure by the red and yellow dots, one of which comes from ψ^* and the other from ψ .

Sinha *et al.* performed a careful series of measurements in which there were three possible paths that a single photon could take through an interferometer. By blocking off various combinations of paths, they measured the contributions from all possible pairs of paths, which were found to contribute at least 99% of the total detection probability. This sets an upper limit of approximately 1% for any contribution from three or more paths, which is consistent with their experimental error. They performed the measurements using true single



Pairwise through many paths. (Left) A single-photon interferometer consists of a source, mirrors, beam splitters, and a detector. Quantum interference only occurs between pairs of optical paths, such as those labeled by the red and yellow dots, as verified in a recent experiment by Sinha *et al.* (Right) A two-photon interferometer (3) is depicted in which quantum interference can occur between sets of four optical paths (where the subscripts L and S refer to long and short paths taken by photons A and B). Quantum interference effects arise regardless of the distance between the interferometers.

Physics Department, University of Maryland Baltimore County, Baltimore, MD 21250, USA. E-mail: jfranson@umbc.edu